



Evolved increases in hemoglobin-oxygen affinity and the Bohr effect coincided with the aquatic specialization of penguins

Anthony V. Signore^{a,1}, Michael S. Tift^b, Federico G. Hoffmann^{c,d}, Todd L. Schmitt^e, Hideaki Moriyama^a, and Jay F. Storz^a

^aSchool of Biological Sciences, University of Nebraska, Lincoln, NE 68588; ^bDepartment of Biology and Marine Biology, University of North Carolina, Wilmington, NC 28403; ^cDepartment of Biochemistry, Molecular Biology, Entomology, and Plant Pathology, Mississippi State University, Starkville, MS 39762; ^dInstitute for Genomics, Biocomputing and Biotechnology, Mississippi State University, Starkville, MS 39762; and ^eVeterinary Services, SeaWorld of California, San Diego, CA 92109

Edited by George N. Somero, Stanford University, Pacific Grove, CA, and approved February 12, 2021 (received for review November 18, 2020)

Dive capacities of air-breathing vertebrates are dictated by onboard O₂ stores, suggesting that physiologic specialization of diving birds such as penguins may have involved adaptive changes in convective O₂ transport. It has been hypothesized that increased hemoglobin (Hb)-O₂ affinity improves pulmonary O₂ extraction and enhances the capacity for breath-hold diving. To investigate evolved changes in Hb function associated with the aquatic specialization of penguins, we integrated comparative measurements of whole-blood and purified native Hb with protein engineering experiments based on site-directed mutagenesis. We reconstructed and resurrected ancestral Hb representing the common ancestor of penguins and the more ancient ancestor shared by penguins and their closest non-diving relatives (order Procellariiformes, which includes albatrosses, shearwaters, petrels, and storm petrels). These two ancestors bracket the phylogenetic interval in which penguin-specific changes in Hb function would have evolved. The experiments revealed that penguins evolved a derived increase in Hb-O₂ affinity and a greatly augmented Bohr effect (i.e., reduced Hb-O₂ affinity at low pH). Although an increased Hb-O₂ affinity reduces the gradient for O₂ diffusion from systemic capillaries to metabolizing cells, this can be compensated by a concomitant enhancement of the Bohr effect, thereby promoting O₂ unloading in acidified tissues. We suggest that the evolved increase in Hb-O₂ affinity in combination with the augmented Bohr effect maximizes both O₂ extraction from the lungs and O₂ unloading from the blood, allowing penguins to fully utilize their onboard O₂ stores and maximize underwater foraging time.

hemoglobin | hypoxia | penguins | Bohr effect | adaptation

In air-breathing vertebrates, diving capacities are dictated by onboard O₂ stores and the efficiency of O₂ use in metabolizing tissues (1). In fully aquatic taxa, selection to prolong breath-hold submergence and underwater foraging time may have promoted adaptive changes in multiple components of the O₂ transport pathway, including oxygenation properties of hemoglobin (Hb). Vertebrate Hb is a tetrameric protein that is responsible for circulatory O₂ transport, loading O₂ in pulmonary capillaries and unloading O₂ in the systemic circulation via quaternary structural shifts between a high-affinity (predominately oxygenated) relaxed (R) state and a low-affinity (predominately deoxygenated) tense (T) state (2). While this mechanism of respiratory gas transport is conserved in all vertebrate Hbs, amino acid variation in the constituent α - and β -type subunits may alter intrinsic O₂ affinity and the responsiveness to changes in temperature, red cell pH, and red cell concentrations of allosteric cofactors (nonheme ligands that modulate Hb-O₂ affinity by preferentially binding and stabilizing the deoxy T conformation) (3, 4).

While the quantity of Hb is typically increased in the blood of diving birds and mammals compared with their terrestrial relatives, there is no consensus on whether evolved changes in

Hb-O₂ affinity have contributed to enhanced diving capacity (1). It has been hypothesized that increased Hb-O₂ affinity may improve pulmonary O₂ extraction in diving mammals, thereby enhancing diving capacity (5), but more comparative data are needed to assess evidence for an adaptive trend (6, 7). Experimental measurements on whole blood suggest that the emperor penguin (*Aptenodytes forsteri*) may have a higher blood-O₂ affinity relative to nondiving waterbirds, a finding that has fostered the view that this is a property characterizing penguins as a group (8–10). However, blood-O₂ affinity is a highly plastic trait that is influenced by changes in red cell metabolism and acid-base balance, so measurements on purified Hb under standard assay conditions are needed to assess whether observed species differences in blood-O₂ affinity stem from genetically based changes in the oxygenation properties of Hb. Moreover, even if species differences in Hb-O₂ affinity are genetically based, comparative data from extant taxa do not reveal whether observed differences are attributable to a derived increase in penguins, a derived reduction in their nondiving relatives, or a combination of changes in both directions.

To investigate evolved changes in Hb function associated with the aquatic specialization of penguins, we integrated experimental measurements of whole-blood and purified native Hb with

Significance

In diving birds like penguins, physiologic considerations suggest that increased hemoglobin (Hb)-O₂ affinity may improve pulmonary O₂ extraction and enhance dive capacity. We integrated experimental tests on whole-blood and native Hbs of penguins with protein engineering experiments on reconstructed ancestral Hbs. The experiments involving ancestral protein resurrection enabled us to test for evolved changes in Hb function in the stem lineage of penguins after divergence from their closest nondiving relatives. We demonstrate that penguins evolved an increased Hb-O₂ affinity in conjunction with a greatly augmented Bohr effect (i.e., reduction in Hb-O₂ affinity at low pH) that should maximize pulmonary O₂ extraction without compromising O₂ delivery at systemic capillaries.

Author contributions: A.V.S. and J.F.S. designed research; A.V.S., M.S.T., F.G.H., T.L.S., and H.M. performed research; M.S.T. and J.F.S. contributed new reagents/analytic tools; A.V.S., M.S.T., F.G.H., H.M., and J.F.S. analyzed data; and A.V.S. and J.F.S. wrote the paper.

The authors declare no competing interest.

This article is a PNAS Direct Submission.

This open access article is distributed under [Creative Commons Attribution License 4.0 \(CC BY\)](https://creativecommons.org/licenses/by/4.0/).

¹To whom correspondence may be addressed. Email: anthony.signore@unl.edu.

This article contains supporting information online at <https://www.pnas.org/lookup/suppl/doi:10.1073/pnas.2023936118/-DCSupplemental>.

Published March 22, 2021.

evolutionary analyses of globin sequence variation. To characterize the mechanistic basis of evolved changes in Hb function in the stem lineage of penguins, we performed protein engineering experiments on reconstructed and resurrected ancestral Hb representing the common ancestor of penguins and the more ancient ancestor shared by penguins and their closest nondiving relatives (order Procellariiformes, which includes albatrosses, shearwaters, petrels, and storm petrels) (Fig. 1). These two ancestors bracket the phylogenetic interval in which penguin-specific changes in Hb function would have evolved.

Results and Discussion

O₂-Binding Properties of Penguin Whole-Blood and Purified Hb. Using blood samples from multiple individuals of six penguin species, we measured the partial pressure of O₂ (PO₂) at 50% saturation (P₅₀) for whole-blood and purified Hb in the absence (stripped) and presence of allosteric cofactors (+KCl +IHP [inositol hexaphosphate]) (Fig. 2). Whole-blood P₅₀ values were similar across all penguins, averaging 33.3 ± 1.1 torr (Fig. 2 and *SI Appendix, Table S1*), consistent with previously published data for emperor, Adélie, chinstrap, and gentoo penguins (8, 9, 11). Similarly, measured O₂ affinities for purified Hb exhibited very little variation among species in both the presence and absence of allosteric cofactors (Fig. 2 and *SI Appendix, Table S1*). Penguins express a single Hb isoform during postnatal life (HbA), in contrast to the majority of other bird species that express one major and one minor isoform (HbA and HbD, respectively) (12, 13). The lack of variation in Hb-O₂ affinity among penguins is consistent with the low level of amino acid variation in the α - and β -chains (*SI Appendix, Fig. S1*). The experiments revealed that penguin Hb exhibits a remarkably large shift in the magnitude of the Bohr effect (i.e., reduced Hb-O₂ affinity in response to reduced pH) with the addition of allosteric cofactors (*SI Appendix, Table S1*). The average Bohr effect of penguin Hbs more than doubles with the addition of allosteric cofactors, from -0.21 ± 0.03 to -0.53 ± 0.04 (*SI Appendix, Table S1*).

Our experimental results indicate that penguins have a generally higher Hb-O₂ affinity than other birds (12, 14–22), consistent with previous suggestions based on measurements of whole blood (8, 9, 23–25). Whole-blood O₂ affinities of the six examined penguin species (30.4 to 38.1 torr at 37 °C, pH 7.40) were uniformly higher than that from a representative member of Procellariiformes, the southern giant petrel (*Macronectes giganteus*; 42.5 torr at 38 °C, pH 7.40) (9). Similarly, numerous high-altitude bird species have convergently evolved increased Hb-O₂ affinities (17, 18, 21), which appears to be adaptive because it helps safeguard arterial O₂ saturation despite the reduced PO₂ of inspired air (26–28). The difference in blood P₅₀ values between penguins and the southern giant petrel is generally much greater in magnitude than differences in Hb P₅₀

between closely related species of low- and high-altitude birds (14–18, 20–22). Similar to the case of other diving vertebrates (29), the Bohr effect of penguin Hb also greatly exceeds typical avian values.

Ancestral Protein Resurrection. In principle, the observed difference in Hb-O₂ affinity between penguins and their closest nondiving relatives could be explained by a derived increase in Hb-O₂ affinity in the penguin lineage (the generally assumed adaptive scenario), a derived reduction in the stem lineage of Procellariiformes (the nondiving sister group), or a combination of changes in both directions. To test these alternative hypotheses, we reconstructed the Hbs of the common ancestor of penguins (AncSphen) and the more ancient common ancestor of Procellariimorphae (the superorder comprising Sphenisciformes [penguins] and Procellariiformes; AncPro) (Fig. 1 and *SI Appendix, Figs. S2–S4*). We then recombinantly expressed and purified the ancestral Hb to perform in vitro functional tests. Measurements of O₂ equilibrium curves revealed that the AncSphen Hb has a significantly higher O₂ affinity than AncPro Hb (Fig. 3), indicating that penguins evolved a derived increase in Hb-O₂ affinity. In the presence of allosteric cofactors, the P₅₀ of AncSphen is much lower (i.e., O₂ affinity is higher) compared to AncPro (11.8 vs. 20.2 torr). Much like the evolved increases in Hb-O₂ affinity in high-altitude birds (18, 20–22, 30), the increased O₂ affinity of penguin Hb is attributable to an increase in intrinsic affinity rather than to reduced responsiveness to allosteric cofactors, as the Hb-O₂ affinity difference between AncSphen and AncPro persists in the presence and absence of Cl⁻ and IHP (Fig. 3).

In addition to the derived increase in Hb-O₂ affinity, comparisons between AncSphen and AncPro also revealed that the Hb of penguins evolved an enhanced responsiveness to pH (Bohr effect). Under stripped conditions, the Bohr effect of AncSphen and AncPro (-0.30 ± 0.09 and -0.27 ± 0.1 , respectively) were highly similar to each other and similar to values measured in native penguin Hb under the same conditions (Fig. 3E and *SI Appendix, Table S1*). However, in the presence of allosteric cofactors, the Bohr effect of AncSphen increased more than two-fold (similar to that of native penguin Hb), whereas that of AncPro showed little change (Fig. 3E), demonstrating that penguins evolved an increased cofactor-linked Bohr effect following divergence from their nondiving relatives. An increased Hb-O₂ affinity is expected to reduce the gradient for O₂ diffusion from systemic capillaries to the cells of metabolizing tissues, and an increased Bohr effect can compensate for this by reducing Hb-O₂ affinity at low pH, thereby promoting O₂ unloading in acidified tissues. A similar augmentation of the Bohr effect was recently documented in the Hb of high-altitude Tibetan canids (31). In summary, the Hb of penguins evolved an increase in O₂ affinity and an enhanced Bohr effect in

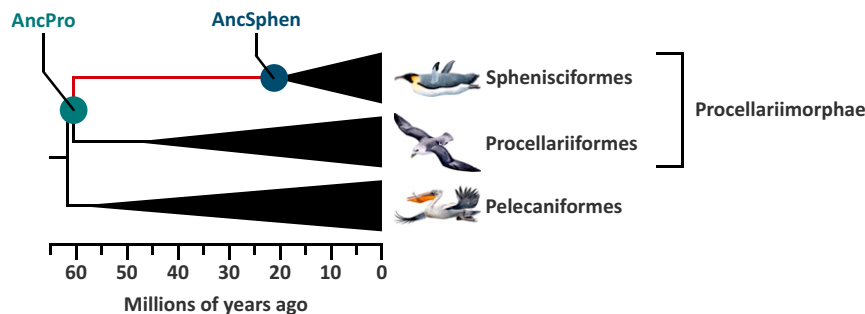


Fig. 1. Diagrammatic phylogeny showing the relationship among Sphenisciformes (penguins), Procellariiformes, and Pelecaniformes. Ancestral Hbs were reconstructed for the two indicated nodes: AncSphen and AncPro (the super order that contains Sphenisciformes and Procellariiformes). Divergence times are adapted from Claramunt and Cracraft (56).

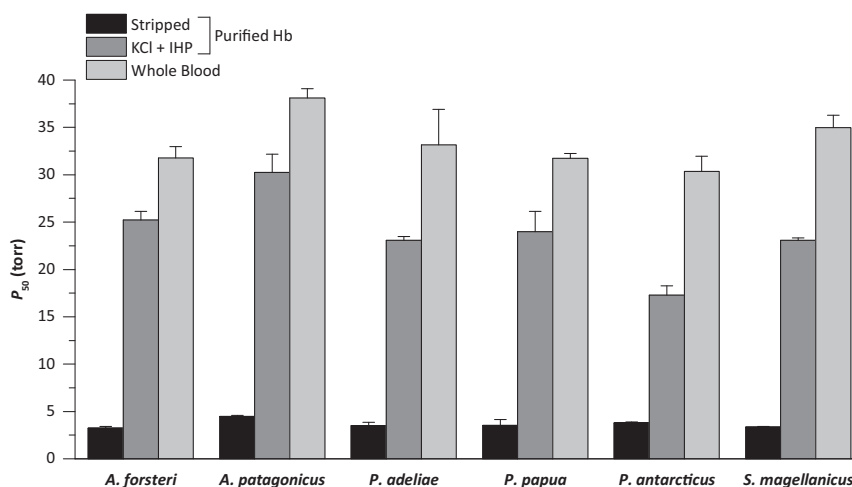


Fig. 2. P_{50} values for penguin whole-blood and purified Hb at 37 °C, in the absence (stripped) and presence of 100 mM KCl and 0.2 mM IHP (+KCl +IHP). The higher the P_{50} , the lower the Hb- O_2 affinity. Whole-blood P_{50} values are presented as mean \pm SE ($n = 3$). Purified Hb P_{50} values are derived from plots of $\log P_{50}$ vs. pH in which a linear regression was fit to estimate P_{50} at exactly pH 7.40 (\pm SE of the regression estimate).

association with other physiologic and morphologic specializations for a more fully aquatic existence.

Tests of Positive Selection. Given that joint increases in the O_2 affinity and Bohr effect of penguin Hb represent derived character states, we performed a molecular evolution analysis to test for evidence of positive selection in the α - and β -globin genes. Specifically, we tested for an accelerated rate of amino acid substitution in the stem lineage of penguins (the branch connecting AncPro to AncSphen) using the branch sites test. This test revealed no evidence for an accelerated rate of amino acid substitution in the stem lineage of penguins (SI Appendix, Table S2), and a clade test revealed no significant variation in the substitution rate among different penguin lineages (SI Appendix, Table S3). Thus, if the increased Hb- O_2 affinity of penguins represents an adaptation that evolved via positive selection, the nature of the causative changes did not produce a detectable statistical signature in the α - and β -type globin genes.

Molecular Modeling. We used molecular modeling to identify which specific amino acid substitutions may be responsible for the increased Hb- O_2 affinity of AncSphen relative to AncPro. Of the 17 amino acid substitutions that distinguish AncSphen and AncPro, our analyses identified four substitutions that could potentially alter O_2 -binding properties. The substitution Thr β 119Ser in the branch leading to AncSphen affects the stabilization of R state (oxygenated) Hb. Specifically, the hydroxyl group of β 119Ser in helix G is oriented toward the subunit interface by forming a hydrogen-bond with β 120Lys, which permits an intersubunit contact with α 111Ile (Fig. 3A and B). This bond between β 119Ser and α 111Ile stabilizes the R state conformation by clamping the intersubunit motions, which is predicted to increase Hb- O_2 affinity by raising the free energy of the oxygenation-linked allosteric R \rightarrow T transition in quaternary structure. Additionally, our model identified three other amino acid substitutions— α A138S, β A51S, and β I55L—that create intersubunit contacts and further stabilize the R state conformation.

Testing Causative Substitutions. To test model-based predictions about the specific substitutions that are responsible for the increased O_2 affinity of penguin Hb, we used site-directed mutagenesis to introduce combinations of mutations at four candidate sites on the AncPro background. We first tested the effect of a single mutation, whereby β 119Thr was replaced with Ser (AncPro β T119S). We then tested the net effect of mutations at

all four sites on the AncPro background (AncPro+4: α A138S, β A51S, β I55L, and β T119S). The protein engineering experiments revealed that β T119S produced a negligible individual effect on Hb- O_2 affinity when introduced on the AncPro background, but produced an appreciable increase in the Bohr effect (Fig. 3D and E). The four mutations in combination produced a modest increase in Hb- O_2 affinity and a more pronounced increase in the Bohr effect, but they did not fully recapitulate the observed differences between AncPro and AncSphen in either of these properties (Fig. 3). These data suggest the evolved functional changes in penguin Hb must be attributable to the net effect of multiple amino acid substitutions at structurally disparate sites.

Adaptive Significance of Increased Hb- O_2 Affinity. The key to extending dive times for aquatic vertebrates is to increase O_2 carrying capacity while keeping metabolic O_2 demands as low as possible during breath-hold submergence. Submergence induces intense bradycardia and peripheral vasoconstriction, which conserves finite O_2 stores for tissues that are intolerant to hypoxia (i.e., the central nervous system and heart) (32–35). O_2 stores are typically increased in diving vertebrates via increased blood volume, increased blood Hb concentration, increased myoglobin concentration in skeletal muscle, increased muscle mass, and, occasionally, increased diving lung volume (1). As deep-diving cetaceans and pinnipeds exhale before submergence, their lungs account for less than 10% of total O_2 stores (1, 36). This reduction in diving lung volume reduces gaseous N_2 and O_2 , which presumably limits decompression sickness. Conversely, as penguins inhale at the onset of a dive, their diving lung volume accounts for a much larger percentage of total O_2 stores (19% for emperor penguins and 45% for Adélie penguins) (1, 37). Indeed, in diving emperor penguins, O_2 extraction from pulmonary stores is continuous during submergence (38, 39). An elevated Hb- O_2 affinity (such as that found in penguins) can maximize O_2 extraction from pulmonary stores, as greater blood O_2 saturation can be achieved at any given parabronchial PO_2 value. However, while increased Hb- O_2 affinity may confer more complete transfer of O_2 from the lungs to the blood, it can inhibit subsequent O_2 transfer from the blood to the tissues. Despite this, emperor penguins deplete their circulatory stores almost completely during extended dives, as their end-of-dive venous PO_2 can be as low as 1 to 6 torr (38). The enhanced Bohr effect of penguin Hb should improve O_2 transport to working (acidic) tissues, allowing more complete O_2 unloading of the blood. We suggest that this modification works in

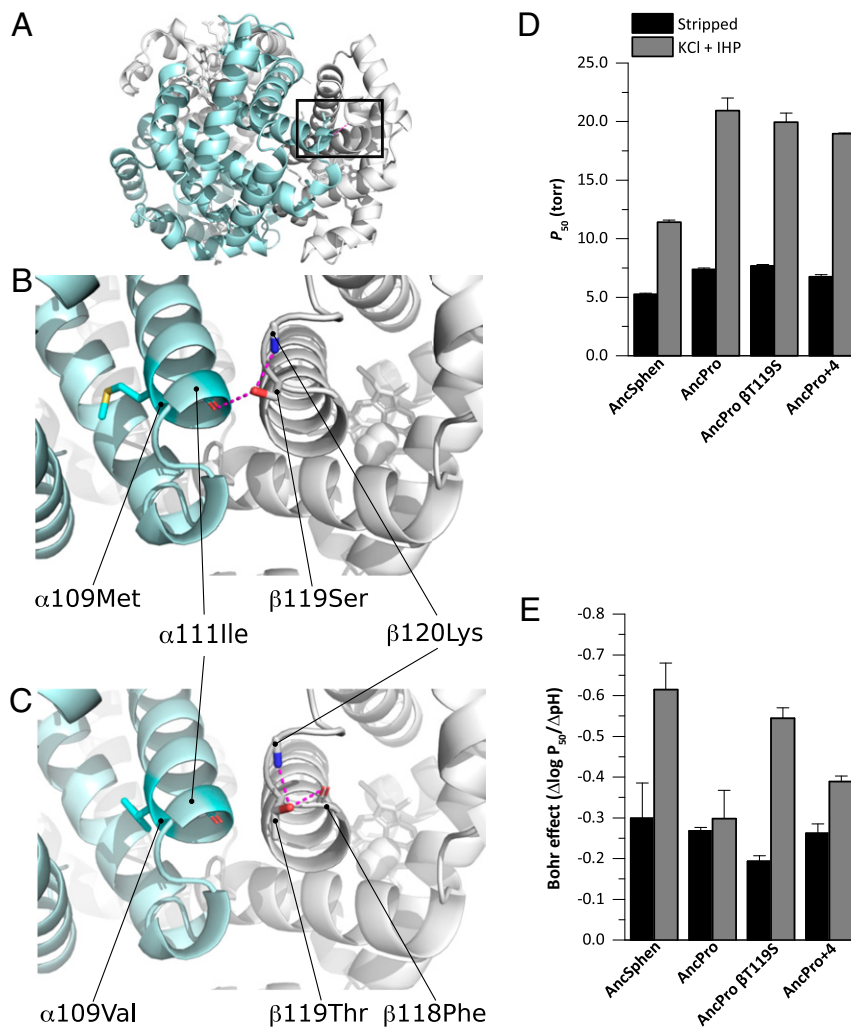


Fig. 3. Structural (A–C) and physiological (D and E) effects of amino acid substitutions in the reconstructed Hb proteins of the penguin ancestor (AncSphen) and the last common ancestor penguins shared with Procellariiformes (AncPro). (A) Molecular model of the AncSphen Hb tetramer, with the black box indicating the regions highlighted in B and C. (B) Molecular model of AncSphen Hb showing intersubunit stabilizing H bonds (pink) between β119Ser and both α111Ile and β120Lys. (C) Molecular model of AncPro Hb showing that replacement of β119Ser with Thr removes the intersubunit stabilizing H bonds. (D) Hb-O₂ affinity (as measured by P₅₀) of AncSphen, AncPro, and two mutant rHbs with penguin-specific amino acid replacements introduced on the AncPro background: AncProβ119Ser and AncPro+4. See the text for an explanation of the choice of candidate sites for mutagenesis experiments. Measurements were performed on Hb solutions (0.1 mM Hb in 0.1 M HEPES/0.5 mM EDTA) at 37 °C in the absence (stripped) and presence of +KCl +IHP. P₅₀ values are derived from plots of logP₅₀ vs. pH, in which a linear regression was fit to estimate P₅₀ at exactly pH 7.40 (± SE of the regression estimate). (E) Bohr coefficients (Δlog P₅₀/ΔpH) were estimated from plots of logP₅₀ vs. pH in which the Bohr effect is represented by the slope of the linear regression (± SE of the slope estimate).

tandem with increased Hb-O₂ affinity to maximize both O₂ extraction from the lungs and O₂ unloading from the blood, allowing penguins to fully utilize their onboard O₂ stores and maximize underwater foraging time.

Materials and Methods

Blood Collection. We collected blood from 18 individual penguins representing six species: *A. forsteri*, *Aptenodytes patagonicus*, *Pygoscelis adeliae*, *Pygoscelis papua*, *Pygoscelis antarcticus*, and *Spheniscus magellanicus* (*n* = 3 individuals per species). All birds were sampled during routine health checks at SeaWorld of California. Blood was collected by venipuncture of the jugular vein using BD Vacutainer Safety-Lok blood collection set with a 21 G × 3/4" (0.8 × 19 mm) needle attached to a heparin blood collection tube (BD). A subsample of whole blood (200 μL) was set aside for oxygen equilibrium curves (see below), and the remaining blood was centrifuged at 5,000 × *g* for 15 min. Plasma, buffy coat, and hematocrit fractions from the centrifuged samples were immediately placed in separate tubes and flash-frozen at –80 °C for future analyses.

Sequencing of Penguin Globin Genes. Globin gene sequencing was performed as described previously (40). In brief, RNA was extracted from ~100 μL of

flash frozen erythrocytes using the Qiagen RNeasy Universal Plus Mini Kit. cDNA was synthesized from freshly prepared RNA using SuperScript IV reverse transcriptase (Invitrogen). Gene-specific primers used to amplify the α- and β-type globin transcripts were designed from the 5' and 3' flanking regions of all publicly available penguin globin genes. PCR reactions were conducted using 1 mL of cDNA template in 0.2-mL tubes containing 25 μL of reaction mixture (0.5 μL of each dNTP [2.5 mM], 2.5 μL of 10X Reaction Buffer [Invitrogen], 0.75 μL of 50 mM MgCl₂, 1.25 μL of each primer [10 pmol/μL], 1 μL of Taq polymerase [Invitrogen], and 16.75 μL of ddH₂O), using an Eppendorf Mastercycler gradient thermocycler. Following a 5-min denaturation period at 94 °C, the desired products were amplified using a cycling profile of 94 °C for 30 s, 53 to 65 °C for 30 s, and 72 °C for 45 s for 30 cycles, followed by a final extension period of 5 min at 72 °C. Amplified products were run on a 1.5% agarose gel, and bands of the correct size were subsequently excised and purified using Zymoclean Gel DNA recovery columns (Zymo Research). Gel-purified PCR products were ligated into pCR4-TOPO vectors using the TOPO TA Cloning Kit and then transformed into One Shot TOP10 chemically competent *Escherichia coli* (Thermo Fisher Scientific). Three to six transformed colonies were cultured in 5 mL of LB medium, and plasmids were subsequently purified with the GeneJET Plasmid Midiprep Kit (Thermo Fisher Scientific). Purified plasmids were sequenced by Eurofins Genomics.

Sequence Analyses. Genomic sequences containing the complete α - and β -globin gene clusters for the emperor penguin (*A. forsteri*), Adélie penguin (*P. adeliae*), northern fulmar (*Fulmarus glacialis*), band-rumped storm petrel (*Hydrobates castro*), southern giant petrel (*M. giganteus*), flightless cormorant (*Nannopterum harrisi*), crested ibis (*Nipponia nippon*), and little egret (*Egretta garzetta*) were obtained from GenBank. The α - and β -globin gene clusters from the remaining 19 extant penguin species were obtained from GigaDB (41). Coding sequences of α - and β -globin genes extracted from these genomic sequences were combined with the newly generated cDNA sequences mentioned above (SI Appendix, Fig. S2). Sequences were aligned using MUSCLE (42) and then used to estimate phylogenetic trees as described previously (40). In brief, the best-fitting codon substitution model and initial tree search were estimated using IQ-TREE with the options -s CODON, -m TESTNEW, -alln, and -bnni (43, 44). Initial trees were then subjected to 1,000 μ ltrafast bootstrap replicates (45). Bootstrap consensus trees (SI Appendix, Fig. S3) were used to estimate ancestral globin sequences using IQ-TREE with the option -asr (SI Appendix, Figs. S2 and S4).

Selection Analyses. We tested for selection in the evolution of the penguins' α - and β -globin genes in a maximum likelihood framework with the codon-based models implemented in the codeml program from the PAML v4.9 suite (46), using the phylogenetic trees described above. We used the branch site and clade models to examine variations in ω , the ratio of the rate of nonsynonymous substitutions per nonsynonymous site, dN, to the rate of synonymous substitutions per synonymous site, dS. We used branch site model A (47, 48) to test for positive selection in the branch connecting AncPro to AncSphen (the stem lineage of penguins) (SI Appendix, Table S2), and used the clade C model (49) to test for selection in the penguin clade using M2a_{rel} from Weadick and Chang (50) as the null model (SI Appendix, Table S3).

Molecular Modeling. Structural modeling was performed on the SWISS MODEL server (51) using graylag goose Hb in oxy form (PDB ID code 1FAW). AncPro Hb and AncSphen Hb had QMEAN values of -0.61 and -0.65 , respectively. A root mean square distance (RMSD) of the main chain between template and model values <0.09 Å was considered usable (52). Structural mining and preparation of graphics were performed using the PyMOL Molecular Graphics System, version 2.3.2 (Schrödinger). Hydrogen bond listing was performed using a PyMOL script list_hb.py (Robert L. Campbell, Biomedical and Molecular Sciences, Queen's University). The interface binding energy was calculated by the ePISA server (53).

Construction of Hb Expression Vectors. Reconstructed ancestral globins were synthesized by GeneArt Gene Synthesis (Thermo Fisher Scientific) after optimizing the nucleotide sequences in accordance with *E. coli* codon preferences. The synthesized globin gene cassette was cloned into a custom pGM vector system along with the methionine aminopeptidase (MAP) gene, as described previously (54). We engineered the Thr β 119Ser substitution by whole-plasmid amplification using mutagenic primers and Phusion High-Fidelity DNA Polymerase (New England BioLabs), phosphorylation with T4 Polynucleotide Kinase (New England BioLabs), and circularization with the NEB Quick Ligation Kit (New England BioLabs). All site-directed mutagenesis steps were performed using the manufacturer's recommended protocol. Each plasmid was verified with DNA sequencing by Eurofins Genomics.

Expression and Purification of Recombinant Hb. Recombinant Hb expression was carried out in the *E. coli* JM109 (DE3) strain as described previously (15, 54, 55). Bacterial cell lysates were loaded onto a HiTrap SP HP anion exchange column (GE Healthcare) and then equilibrated with 50 mM Hepes/0.5 mM EDTA (pH 7.0) and eluted with a linear gradient of 0 to 0.25 M NaCl. Hb-containing fractions were then loaded onto a HiTrap Q HP cation exchange column (GE Healthcare) equilibrated with 20 mM Tris-HCl/0.5 mM

EDTA (pH 8.6) and eluted with a linear pH gradient of 0 to 0.25 M NaCl. Eluted Hb fractions were concentrated using Amicon Ultra-4 Centrifugal Filter Units (EMD Millipore).

Sample Preparation for O₂ Equilibrium Curves. Fresh whole blood was diluted 1:15 with each individual's own plasma, and O₂ equilibrium curves were measured immediately after sampling. To obtain stripped hemolysate, 100 μ L of centrifuged red blood cells were added to a 5 \times volume of 0.01 M Hepes/0.5 mM EDTA buffer (pH 7.4), followed by a 30-min incubation on ice to lyse the red blood cells. NaCl was added to a final concentration of 0.2 M, and samples were centrifuged at 20,000 \times g for 10 min to remove cell debris. Hemolysate supernatants and purified recombinant Hb were similarly desalted by passing through a PD-10 desalting column (GE Healthcare) equilibrated with 25 mL of 0.01 M Hepes/0.5 mM EDTA (pH 7.4). Eluates were concentrated using Amicon Ultra-4 Centrifugal Filter Units (EMD Millipore). From these concentrated samples, Hb solutions (0.1 mM Hb in 0.1 M Hepes/0.05 M EDTA buffer) were prepared in the absence (stripped) and the presence of 0.1 M KCl and 0.2 mM inositol hexaphosphate (+KCl +IHP). Stripped and +KCl +IHP treatments were prepared at three different pH values (for a total of six treatments per Hb sample). Working solutions were adjusted with NaOH to as close to pH 7.2, 7.4, or 7.6 as possible, and then pH was precisely measured with an Orion Star A211 pH Meter and Orion PerpHecT ROSS Combination pH Micro Electrode (Thermo Fisher Scientific).

Measuring O₂-Binding Properties. O₂ equilibrium curves were measured using a blood oxygen-binding system (BOBS; Loligo Systems) at 37 °C. The pH of whole-blood samples was set by measuring curves in the presence of 45 torr CO₂, whereas the pH of Hb solutions was set with Hepes buffer (see above). Each whole-blood sample and Hb solution was sequentially equilibrated with an array of oxygen tensions (PO₂), while the sample absorbance was continually monitored at 430 nm (deoxy peak) and 421 nm (oxy/deoxy isobestic point). Each equilibration step was considered complete when the absorbance at 430 nm had stabilized (2 to 4 min). Only PO₂ values yielding 30 to 70% Hb O₂ saturation were used in subsequent analyses. Hill plots ($\log[\text{fractional saturation}/(1 - \text{fractional saturation})]$ vs. $\log\text{PO}_2$) were constructed from these measurements. A linear regression was fitted to these plots and used to determine the PO₂ at half-saturation (P₅₀) and the cooperativity coefficient (n₅₀), where the x-intercept and slope of the regression line represent the P₅₀ and n₅₀, respectively. Values for whole-blood samples (n = 3) are presented as mean \pm SE. For Hb solutions, a linear regression was fit to plots of $\log\text{P}_{50}$ vs. pH, and the resulting equation was used to estimate P₅₀ values at pH 7.40 (\pm SE of the regression estimate). We did not make direct comparisons between native Hb and recombinantly expressed Hb, because recombinant Hb often exhibits slightly lower P₅₀ values due to an increased rate of autoxidation. Thus, all inferences are based on comparisons among native Hb samples from extant species or on comparisons between recombinant Hb samples representing reconstructed ancestors.

Data Availability. All study data are included in the main text and SI Appendix.

ACKNOWLEDGMENTS. We thank the trainers and veterinary staff at SeaWorld of California for their help with this project, Jennifer Rego for blood sample collection, and Dr. Judy St. Leger for logistical support. We also thank S. Mohammadi, N. Gutierrez-Pinto, J. Hite, M. Kobiela, A. Dhawanjewar, M. Kulbaba, M. Gaudry, and A. Quijada-Rodriguez for helpful comments on the manuscript. This research was supported by funding from the NIH (HL087216, to J.F.S. and F32HL136202, to M.S.T.), the NSF (OIA-1736249, to J.F.S.; IOS-1927675, to J.F.S.; and 1927616, to M.S.T.) and a SeaWorld Parks & Entertainment technical contribution (2020-19).

- G. L. Kooyman, P. J. Ponganis, The physiological basis of diving to depth: Birds and mammals. *Annu. Rev. Physiol.* **60**, 19–32 (1998).
- M. F. Perutz, Stereochemistry of cooperative effects in haemoglobin. *Nature* **228**, 726–739 (1970).
- M. F. Perutz, Species adaptation in a protein molecule. *Mol. Biol. Evol.* **1**, 1–28 (1983).
- J. F. Storz, *Hemoglobin: Insights into Protein Structure, Function, and Evolution* (Oxford University Press, 2019).
- G. K. Snyder, Respiratory adaptations in diving mammals. *Respir. Physiol.* **54**, 269–294 (1983).
- A. V. Signore et al., Emergence of a chimeric globin pseudogene and increased hemoglobin oxygen affinity underlie the evolution of aquatic specializations in Sirenia. *Mol. Biol. Evol.* **36**, 1134–1147 (2019).
- M. S. Tift, P. J. Ponganis, Time domains of hypoxia adaptation—elephant seals stand out among divers. *Front. Physiol.* **10**, 677 (2019).
- J. U. Meir, P. J. Ponganis, High-affinity hemoglobin and blood oxygen saturation in diving emperor penguins. *J. Exp. Biol.* **212**, 3330–3338 (2009).
- W. K. Milsom, K. Johansen, R. W. Millard, Blood respiratory properties in some Antarctic birds. *Condor* **75**, 472–474 (1973).
- B. Wienecke, G. Robertson, R. Kirkwood, K. Lawton, Extreme dives by free-ranging emperor penguins. *Polar Biol.* **30**, 133–142 (2007).
- C. Lenfant, G. L. Kooyman, R. Elsner, C. M. Drabek, Respiratory function of blood of the Adélie penguin *Pygoscelis adeliae*. *Am. J. Physiol.* **216**, 1598–1600 (1969).
- M. T. Grispo et al., Gene duplication and the evolution of hemoglobin isoform differentiation in birds. *J. Biol. Chem.* **287**, 37647–37658 (2012).
- J. C. Opazo et al., Gene turnover in the avian globin gene families and evolutionary changes in hemoglobin isoform expression. *Mol. Biol. Evol.* **32**, 871–887 (2015).

14. J. Projecto-García *et al.*, Repeated elevational transitions in hemoglobin function during the evolution of Andean hummingbirds. *Proc. Natl. Acad. Sci. U.S.A.* **110**, 20669–20674 (2013).
15. Z. A. Cheviron *et al.*, Integrating evolutionary and functional tests of adaptive hypotheses: A case study of altitudinal differentiation in hemoglobin function in an Andean sparrow, *Zonotrichia capensis*. *Mol. Biol. Evol.* **31**, 2948–2962 (2014).
16. S. C. Galen *et al.*, Contribution of a mutational hot spot to hemoglobin adaptation in high-altitude Andean house wrens. *Proc. Natl. Acad. Sci. U.S.A.* **112**, 13958–13963 (2015).
17. C. Natarajan *et al.*, Convergent evolution of hemoglobin function in high-altitude Andean waterfowl involves limited parallelism at the molecular sequence level. *PLoS Genet.* **11**, e1005681 (2015).
18. C. Natarajan *et al.*, Predictable convergence in hemoglobin function has unpredictable molecular underpinnings. *Science* **354**, 336–339 (2016).
19. A. Kumar *et al.*, Stability-mediated epistasis restricts accessible mutational pathways in the functional evolution of avian hemoglobin. *Mol. Biol. Evol.* **34**, 1240–1251 (2017).
20. A. Jendroszek *et al.*, Allosteric mechanisms underlying the adaptive increase in hemoglobin-oxygen affinity of the bar-headed goose. *J. Exp. Biol.* **221**, jeb185470 (2018).
21. X. Zhu *et al.*, Divergent and parallel routes of biochemical adaptation in high-altitude passerine birds from the Qinghai-Tibet Plateau. *Proc. Natl. Acad. Sci. U.S.A.* **115**, 1865–1870 (2018).
22. C. Natarajan *et al.*, Molecular basis of hemoglobin adaptation in the high-flying bar-headed goose. *PLoS Genet.* **14**, e1007331 (2018).
23. E. H. Christensen, B. Dill, Oxygen dissociation curves of bird blood. *J. Biol. Chem.* **109**, 443–448 (1935).
24. F. H. Baumann, R. Baumann, A comparative study of the respiratory properties of bird blood. *Respir. Physiol.* **31**, 333–343 (1977).
25. P. Lutz, On the oxygen affinity of bird blood. *Am. Zool.* **1**, 187–198 (1980).
26. J. F. Storz, Hemoglobin-oxygen affinity in high-altitude vertebrates: Is there evidence for an adaptive trend? *J. Exp. Biol.* **219**, 3190–3203 (2016).
27. J. F. Storz, G. R. Scott, Life ascending: Mechanism and process in physiological adaptation to high-altitude hypoxia. *Annu. Rev. Ecol. Syst.* **50**, 503–526 (2019).
28. K. B. Tate *et al.*, Circulatory mechanisms underlying adaptive increases in thermogenic capacity in high-altitude deer mice. *J. Exp. Biol.* **220**, 3616–3620 (2017).
29. C. Lenfant, K. Johansen, J. D. Torrance, Gas transport and oxygen storage capacity in some pinnipeds and the sea otter. *Respir. Physiol.* **9**, 277–286 (1970).
30. J. U. Meir, W. K. Millsom, High thermal sensitivity of blood enhances oxygen delivery in the high-flying bar-headed goose. *J. Exp. Biol.* **216**, 2172–2175 (2013).
31. A. V. Signore *et al.*, Adaptive changes in hemoglobin function in high-altitude Tibetan canids were derived via gene conversion and introgression. *Mol. Biol. Evol.* **36**, 2227–2237 (2019).
32. P. J. Butler, D. R. Jones, Physiology of diving of birds and mammals. *Physiol. Rev.* **77**, 837–899 (1997).
33. P. J. Butler, A. J. Woakes, Heart rate and aerobic metabolism in Humboldt penguins, *Spheniscus humboldti*, during voluntary dives. *J. Exp. Biol.* **108**, 419–428 (1984).
34. J. U. Meir, T. K. Stockard, C. L. Williams, K. V. Ponganis, P. J. Ponganis, Heart rate regulation and extreme bradycardia in diving emperor penguins. *J. Exp. Biol.* **211**, 1169–1179 (2008).
35. G. Froget *et al.*, Heart rate and energetics of free-ranging king penguins (*Aptenodytes patagonicus*). *J. Exp. Biol.* **207**, 3917–3926 (2004).
36. P. J. Ponganis, Diving mammals. *Compr. Physiol.* **1**, 447–465 (2011).
37. G. L. Kooyman, J. P. Schroeder, D. G. Greene, V. A. Smith, Gas exchange in penguins during simulated dives to 30 and 68 m. *Am. J. Physiol.* **225**, 1467–1471 (1973).
38. P. J. Ponganis *et al.*, Returning on empty: Extreme blood O₂ depletion underlies dive capacity of emperor penguins. *J. Exp. Biol.* **210**, 4279–4285 (2007).
39. P. J. Ponganis *et al.*, O₂ store management in diving emperor penguins. *J. Exp. Biol.* **212**, 217–224 (2009).
40. A. V. Signore, J. F. Storz, Biochemical pedomorphosis and genetic assimilation in the hypoxia adaptation of Tibetan antelope. *Sci. Adv.* **6**, eabb5447 (2020).
41. H. Pan *et al.*, High-coverage genomes to elucidate the evolution of penguins. *Giga-science* **8**, giz117 (2019).
42. R. C. Edgar, MUSCLE: Multiple sequence alignment with high accuracy and high throughput. *Nucleic Acids Res.* **32**, 1792–1797 (2004).
43. L.-T. Nguyen, H. A. Schmidt, A. von Haeseler, B. Q. Minh, IQ-TREE: A fast and effective stochastic algorithm for estimating maximum-likelihood phylogenies. *Mol. Biol. Evol.* **32**, 268–274 (2015).
44. S. Kalyaanamoorthy, B. Q. Minh, T. K. F. Wong, A. von Haeseler, L. S. Jermini, ModelFinder: Fast model selection for accurate phylogenetic estimates. *Nat. Methods* **14**, 587–589 (2017).
45. D. T. Hoang, O. Chernomor, A. von Haeseler, B. Q. Minh, L. S. Vinh, UFBoot2: Improving the ultrafast bootstrap approximation. *Mol. Biol. Evol.* **35**, 518–522 (2018).
46. Z. Yang, PAML 4: Phylogenetic analysis by maximum likelihood. *Mol. Biol. Evol.* **24**, 1586–1591 (2007).
47. J. Zhang, R. Nielsen, Z. Yang, Evaluation of an improved branch-site likelihood method for detecting positive selection at the molecular level. *Mol. Biol. Evol.* **22**, 2472–2479 (2005).
48. Z. Yang, S. Kumar, M. Nei, A new method of inference of ancestral nucleotide and amino acid sequences. *Genetics* **141**, 1641–1650 (1995).
49. J. P. Bielawski, Z. Yang, A maximum likelihood method for detecting functional divergence at individual codon sites, with application to gene family evolution. *J. Mol. Evol.* **59**, 121–132 (2004).
50. C. J. Weadick, B. S. W. Chang, An improved likelihood ratio test for detecting site-specific functional divergence among clades of protein-coding genes. *Mol. Biol. Evol.* **29**, 1297–1300 (2012).
51. A. Waterhouse *et al.*, SWISS-MODEL: Homology modelling of protein structures and complexes. *Nucleic Acids Res.* **46**, W296–W303 (2018).
52. P. Benkert, M. Biasini, T. Schwede, Toward the estimation of the absolute quality of individual protein structure models. *Bioinformatics* **27**, 343–350 (2011).
53. E. Krissinel, K. Henrick, Inference of macromolecular assemblies from crystalline state. *J. Mol. Biol.* **372**, 774–797 (2007).
54. C. Natarajan *et al.*, Expression and purification of recombinant hemoglobin in *Escherichia coli*. *PLoS One* **6**, e20176 (2011).
55. C. Natarajan *et al.*, Epistasis among adaptive mutations in deer mouse hemoglobin. *Science* **340**, 1324–1327 (2013).
56. S. Claramunt, J. Cracraft, A new time tree reveals Earth history's imprint on the evolution of modern birds. *Sci. Adv.* **1**, e1501005 (2015).